The Journal of Chemical Physics

# Non-Hermitian quantum mechanics and exceptional points in molecular electronics

Cite as: J. Chem. Phys. **152**, 244119 (2020); https://doi.org/10.1063/5.0006365
Submitted: 01 March 2020 . Accepted: 11 June 2020 . Published Online: 26 June 2020

Matthias Ernzerhof, Alexandre Giguère, and Didier Mayou



The Journal of Chemical Physics ARTICLE scitation.org/journal/jcp

# Non-Hermitian quantum mechanics and exceptional points in molecular electronics

Cite as: J. Chem. Phys. 152, 244119 (2020); doi: 10.1063/5.0006365
Submitted: 1 March 2020 • Accepted: 11 June 2020 •
Published Online: 26 June 2020



Matthias Ernzerhof,[1,a] Alexandre Giguère,[1,2] and Didier Mayou[3]

## AFFILIATIONS

[1] Département de Chimie, Université de Montréal, C.P. 6128 Succursale A, Montréal, Québec H3C 3J7, Canada
[2] Département des Sciences de la Nature, Collège Militaire Royal de Saint-Jean, Saint-Jean-sur-Richelieu, Québec J3B 8R8, Canada
[3] Institut Néel, 25 Avenue des Martyrs, BP 166, 38042 Grenoble Cedex 9, France

[a] **Author to whom correspondence should be addressed:** Matthias.Ernzerhof@UMontreal.ca

## ABSTRACT

In non-Hermitian (NH) quantum mechanics, Hamiltonians are studied whose eigenvalues are not necessarily real since the condition of hermiticity is not imposed. Certain symmetries of NH operators can ensure that some or all of the eigenvalues are real and thus suitable for the description of physical systems whose energies are always real. While the mathematics of NH quantum mechanics is well developed, applications of the theory to real quantum systems are scarce, and no closed system is known whose Hamiltonian is NH. Here, we consider the elementary textbook example of a NH Hamiltonian matrix, and we show how it naturally emerges as a simplifying concept in the modeling of molecular electronic devices. We analyze the consequences of non-Hermiticity and exceptional points in the spectrum of NH operators for the molecular conductance and the spectral density of simple models for molecules on surfaces.



## I. INTRODUCTION

Non-Hermitian (NH) quantum mechanics (QM),[1–4] where the Hamiltonian operator describing the system of interest is not Hermitian, has become a subject of considerable interest. Non-Hermitian Hamiltonians appear in numerous areas of molecular sciences; some examples are scattering theory,[3,5,6] molecular resonances,[7–11] electronic structure theory,[1,2,9,12–15] Green's function theory,[16–18] and modern optics.[4,19] Often, parameter-dependent NH Hamiltonians are studied whose spectrum changes gradually as the parameter changes, with real eigenvalues converting into complex ones. At the transition point, referred to as the exceptional point,[2,20–22] two eigenvalues coalesce with coalescing eigenvectors. This implies that the Hamiltonian is not diagonalizable any more according to the mathematical definition. The physical significance of such exceptional points is one of the questions that we address here.

An example of a NH Hamiltonian that is often discussed in the literature[23] is

$$\mathcal{H} = -\frac{d^2}{dx^2} + ix^3. \tag{1}$$

All the eigenvalues of this Hamiltonian are real, but it is obviously not Hermitian; it belongs to the class of parity (P) and time (T) inversion symmetric operators. Parity inversion leads to a minus sign in the potential, and subsequent time inversion, which changes $i$ to $-i$ in $H$, yields back the initial Hamiltonian.

While NH Hamiltonians with real eigenvalues appear to be suitable for the description of physical systems whose energies are always real, there is, to the best of our knowledge, no closed quantum system whose Hamiltonian is non-Hermitian. Here, we provide a direct connection of NHQM to open physical systems. To do so, we stay within the matrix representation of NHQM. The simplest NH Hamiltonian matrix is

$$H = \begin{pmatrix} i\beta & \beta_M \\ \beta_M & -i\beta \end{pmatrix}, \tag{2}$$

and it is the textbook example of a NH Hamiltonian matrix and provides the starting point for many developments in NHQM. It is this Hamiltonian that we relate to a physical, quantum mechanical problem. To be more specific, we show that this matrix appears in a mathematical model of a molecular electronic device (MED),[24–31]

and it provides access to the electrical conductance of a diatomic molecule.

One of the interesting aspects of NHQM is the appearance of exceptional points, and $H$ of Eq. (2) serves to illustrate them. The eigenvalues of $H$ are given by

$$E_{1,2} = \pm\sqrt{\beta_M^2 - \beta^2}, \tag{3}$$

and the associated eigenvectors are

$$v_{1,2} = \left(\frac{\pm\sqrt{\beta_M^2 - \beta^2} + i\beta}{\beta_M}, 1\right). \tag{4}$$

Apparently, for $|\beta_M| > |\beta|$, the eigenvalues are real and the corresponding eigenvectors are distinct. However, when $|\beta_M| = |\beta|$, the eigenvalues coalesce and their eigenvectors coalesce as well,

$$v_{1,2} = (i, 1) \quad \text{for } \beta_M = \beta, \tag{5}$$

a peculiar behavior that is a defining characteristic for an exceptional point. For $|\beta_M| < |\beta|$, the eigenvalues are complex conjugate and purely imaginary values. The corresponding eigenvectors have coefficients with unequal absolute values, whereas before reaching the exceptional point, the absolute values of the coefficients are equal. In the present work, we relate exceptional points of the NH Hamiltonian matrix to measurable properties of MEDs.

Maybe the most widespread application of the NH theory can be found in modern optics.[4,19] This is not an actual realization of NHQM, however, since the underlying equations, which are reformulated in terms of NH operators, are the Maxwell equations. There are realizations of NHQM in open physical systems in whose description complex potentials are employed to model the external reservoirs.[3,32–35] The imaginary part in these complex potentials simulates the transfer of probability density into and out of the system. The incarnation of NHQM that we focus on in the present contribution also employs external reservoirs; in the MEDs we consider, molecules are coupled to two external contacts and a current is transferred through the molecule from one reservoir to the other.

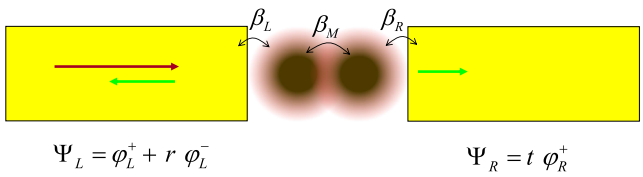


**FIG. 1.** Schematic representation of a diatomic molecule coupled to metal contacts. Using a simple Hückel description of the molecular electronic device, the coupling coefficient between the atoms is $\beta_M$ and the coupling coefficients to the left and right contact are $\beta_L$ and $\beta_R$, respectively. Note that no contact atoms are displayed since in our mathematical model, the contacts are considered as a featureless continuum with constant density of states; the molecular atoms, however, are considered explicitly. The imposed boundary conditions are that there is an incoming electron wave $\varphi_L^+$ in the left contact that is partially reflected into $\varphi_L^-$ at the contact–molecule interface. The corresponding reflection coefficient is $r$. In the right contact, there is only an outgoing electron wave $\varphi_R^+$ that is weighted by the transmission amplitude $t$. Modeling the contacts through complex potentials yields NH Hamiltonian matrices, as shown in Sec. II.

A sketch of a MED is provided in Fig. 1. Often, Green's function based formalisms (e.g., Refs. 24, 31, and 36–39) are invoked to describe MEDs and to calculate their conductance; in these methods, effective Hamiltonians are employed that are also non-Hermitian. In general, however, they are not PT symmetric, have no real eigenvalues, and do not exhibit exceptional points. In the following, we review the source-sink potential (SSP) approach[40,41] for the conductance of MEDs in which the Hamiltonian matrix Eq. (2) plays a key role. This enables us to concisely discuss molecular conductance in terms of NHQM. In addition, we adapt the SSP model to describe molecules bound to surfaces. We describe these systems in terms of NH Hamiltonians and identify observable consequences of exceptional points.

## II. NON-HERMITIAN HAMILTONIANS FOR MOLECULAR ELECTRONIC DEVICES

Molecular electronic devices described within the source-sink potential method (SSP) provide an abundant source of NH Hamiltonians that, by construction, exhibit real eigenvalues.[40,41] Interestingly, these Hamiltonians are, in general, not PT symmetric except for MEDs with a mirror plane perpendicular through the molecular conductor. In the following, we review the simplest version of the SSP model and we discuss basic aspects of NH Hamiltonians, which help develop an interpretation of these operators. The first step toward a physical interpretation of an imaginary contribution to the Hamiltonian is the continuity equation.

### A. Continuity equation

For the present purposes, we are particularly interested in the matrix version of the continuity equation. To be specific and also for later use, we consider a Hamiltonian matrix that describes a diatomic molecule that is attached to a surface through one of its atoms; this arrangement is depicted in Fig. 2 and its model Hamiltonian is given by

$$H = \begin{pmatrix} 0 & \beta_M \\ \beta_M & -i\beta \end{pmatrix}. \tag{6}$$

Invoking the usual steps, i.e., using the time-dependent Schrödinger equation to calculate the time derivative of the electron density, we arrive at

$$\frac{d}{dt} c_k^* c_k = i\left(c_k^* \beta_M c_l - c_k \beta_M c_l^*\right) - 2c_k^* \beta \delta_{2,k} c_k. \tag{7}$$

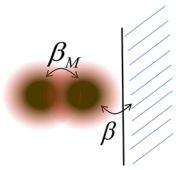


$$H = \begin{pmatrix} 0 & \beta_M \\ \beta_M & -i\beta \end{pmatrix}$$

**FIG. 2.** Schematic representation of a diatomic molecule attached to a surface through one of its atoms. The coupling coefficient between the atoms is $\beta_M$, and the coupling to the continuum of states of the surface is $\beta$. The NH Hamiltonian matrix modeling this system is displayed on the right-hand side. The derivation of this Hamiltonian is provided through the source-sink potential model in Sec. IV.

The absolute value squared on the left-hand side represents the probability density on site $k = 1, 2$. The probability density changes as a function of time, and on site one, its time derivative is given by $i\left(c_1^*\beta_M c_2 - c_1\beta_M c_2^*\right)$, which is the current flowing from site one to site two. The negative of this term appears in the time derivative of the probability density on site two. In addition, on site two, this probability density diminishes over time at a rate set by the coefficient $\beta$. Inversion of the sign of $\beta$, yielding a positive imaginary term in the Hamiltonian, turns this sink of probability density into a source of it. This complex conjugation of the potential results in complex conjugation of the eigenfunction and inversion of the direction of probability current flow between the atoms.

The current from site one to site two is proportional to the coefficient $\beta_M$, showing that this coefficient limits the current flow between atoms. This observation helps us to understand the appearance of complex eigenvalues of the Hamiltonian Eq. (2); the current that can be transported from one site to the next is limited by $\beta_M$, and trying to push and pull more current through the system by means of increasing $\beta$ leads to an accumulation of probability density on one site and a depletion of probability density on the other site. This depletion and accumulation manifests itself in imaginary parts of the eigenvalues of negative or positive sign, respectively, showing that the norm of the corresponding wave function is exponentially decreasing or increasing as time evolves.[41]

### B. Wide-band limit of the source-sink potential (SSP) model

The source-sink potential (SSP) method was developed[40–49] in the context of the tight-binding, or equivalently, the Hückel model. Subsequently, it has also been extended[43,50,51] to advanced electronic structure methods such as Kohn–Sham density functional theory and Hartree–Fock theory. The SSP formalism has been shown to be equivalent[44] to the Green's function approach for molecular conductance,[24,31,36–39] and it has been re-derived and reformulated.[42,47] Examples of molecular conductors very similar to the ones considered here have been treated analytically within the Green's function approach in Ref. 39, and no exceptional points are observed in the model Hamiltonians.

Instead of reviewing SSP, here, we present a short summary of the simplest version[40] of SSP where one-dimensional, semi-infinite contacts in the wideband limit (WBL) are considered. A sketch of a MED is provided in Fig. 1. In the left contact, an electron wave is arriving with an energy $E$, and upon reaching the molecule, it is partially reflected. The corresponding reflection coefficient is given by $r(E)$; it is a function of the incident electron energy $E$. The isolated molecule has discrete energy levels, which, upon hybridization with the contacts, modulate the coefficient $r(E)$. In the SSP model, the left contact is rigorously accounted for by the source potential $\sigma_{\mathrm{L}}(r)$, which is added to the diagonal matrix element of the atom to which the left contact is attached to. The right contact, also a linear chain of atoms in the WBL, carries only an outgoing electron wave, and it is accounted for by a sink potential $\sigma_{\mathrm{R}}$, which is a mere constant under the described conditions. The simplest model for a diatomic molecule is defined through the Hückel matrix,

$$H_M = \begin{pmatrix} h_a & \beta_{\mathrm{M}} \\ \beta_{\mathrm{M}} & h_b \end{pmatrix}, \tag{8}$$

with on-site energies $h_a$ and $h_b$ and site–site coupling $\beta_M$. Coupling the molecule to external contacts, modeled through source and sink potentials, yields

$$H(r) = \begin{pmatrix} h_a + \beta_L\sigma_{\mathrm{L}}(r) & \beta_{\mathrm{M}} \\ \beta_{\mathrm{M}} & h_b + \beta_R\sigma_{\mathrm{R}} \end{pmatrix}, \tag{9}$$

where

$$\sigma_{\mathrm{L}}(r) = i\frac{1+r}{1-r} \tag{10}$$

and

$$\sigma_{\mathrm{R}} = -i. \tag{11}$$

As opposed to the SSP for finite bandwidth contacts where the model Hamiltonian depends on the electron energy explicitly in addition to the dependence through the reflection coefficient, i.e., $H = H(E, r(E))$, in the WBL, the operator $H$ depends on $r(E)$ solely.[40] According to the continuity equation,[41,52] the imaginary part of the potentials acts as source or sink of current density, depending on whether the sign of the imaginary part is positive or negative, respectively. Obviously, in $H(r(E))$, the left contact is modeled by a source and the right contact by a sink term. To obtain the projection of the device wave function onto the molecular subspace, one has to choose an energy $E$, plug the reflection coefficient $r(E)$ into $H$ of Eq. (9), and calculate its eigenvector of energy $E$. Since the boundary condition of having an incoming electron wave in the left contact is built into $H(r(E))$, the eigenvectors obtained are not those of the effective Hamiltonian of Green's function theory (cf. Ref. 39).

### C. Factorization of the reflection coefficient

To obtain $r(E)$, we start with a given value of the energy and consider the matrix eigenvalue equation yielding this energy,

$$H(r(E))C_{\mathrm{M}} = EC_{\mathrm{M}}. \tag{12}$$

The eigenvector $C_{\mathrm{M}}$ is of the dimension of the molecular Hückel matrix and it represents the molecular part of the MED wave function. We form the characteristic polynomial $P(E)$ of $H(r(E))$ and impose the condition satisfied for each eigenvalue $E$,

$$\begin{aligned} P(E) &= \mathrm{Det}[H(r(E)) - E] \\ &= 0. \end{aligned} \tag{13}$$

This represents an implicit equation for $r(E)$, which is the only unknown in it. Because of the algebraic nature of our model, using Eq. (13), $r(E)$ can be obtained as a rational function of $E$ of the form[40]

$$r(E) = \frac{a_0 + a_1E + a_2E^2 + \cdots + a_NE^N}{b_0 + b_1E + b_2E^2 + \cdots + b_NE^N}, \tag{14}$$

where $N$ is the dimension of $H(r)$. According to the fundamental theorem of algebra, Eq. (14) can be recast,

$$r(E) = c\frac{(E_1^{trns} - E)(E_2^{trns} - E)\cdots(E_N^{trns} - E)}{(E_1^{abs} - E)(E_2^{abs} - E)\cdots(E_N^{abs} - E)}. \tag{15}$$

Here, $c$ is a constant that we determine by imposing the condition $\lim_{|E|\to\infty}|r(E)| = 1$, which results in $c = 1$. Focusing on the numerator in the expression for $r(E)$, clearly, the set $\{E_i^{trns}\}_{i=1,\ldots,N}$ is the set of energies for which the reflection coefficient vanishes.[40] Therefore, this set is given by the eigenvalues of the Hamiltonian

$$H^{trns} = H(r = 0). \tag{16}$$

We refer to $H^{trns}$ as the transparent Hamiltonian. Similarly, the set of values $\{E_i^{abs}\}_{i=1,\ldots,N}$ corresponds to the poles in the function $r(E)$, which are obtained as eigenvalues of

$$H^{abs} = H(|r| = \infty). \tag{17}$$

For $|r| = \infty$, the artificial potential for the left contact becomes identical to its counterpart in the right contact; both are absorbing.[41] Consequently, we refer to the eigenstates of $H^{abs}$ as the decaying states. Clearly, their energy has a negative imaginary part, indicating a finite lifetime. It is worth noting that the model Hamiltonian of the Green's function approach to molecular conductance coincides with $H^{abs}$.[39] Furthermore, we emphasize that the numerator and the denominator of Eq. (15) are the characteristic polynomials of the operators $H(r = 0)$ and $H(|r| = \infty)$. Therefore,

$$r(E) = \frac{\mathrm{Det}[H^{trns} - E]}{\mathrm{Det}[H^{abs} - E]}. \tag{18}$$

Equations (15) and (18) represent the reflection coefficient $r(E)$ in terms of eigenvalues of NH Hamiltonians or in terms of NH Hamiltonians, respectively. The states of the MED form a continuum, whereas the spectrum of the NH Hamiltonians is discrete—a fact that greatly simplifies the determination and analysis of $r(E)$. The reflection coefficient contains the information necessary to determine the physical properties of the system. Together with $H(r(E))$, it enables one to construct the continuum wave functions of the system as a linear combination of incoming and reflected waves in the left contact, the outgoing wave in the right contact, and the molecular part of the wave function obtained with $H(r(E))$.

## III. TRANSMISSION PROBABILITY OF A DIATOMIC MOLECULE CONNECTED TO CONTACTS

The SSP method and the described factorization of $r(E)$ can be employed to study the conductance of arbitrary complex molecules described within the Hückel approximation. However, to reveal the relation of SSP to NHQM, it suffices to consider a simple example of a diatomic molecule connected to external contacts as described in Sec. II B.

To further simplify the Hamiltonian matrix in Eq. (9), we set the energies of the separated atoms to zero, and we assume that $\beta_L = \beta_R = \beta$, yielding

$$H(r(E)) = \begin{pmatrix} i\beta\frac{1+r}{1-r} & \beta_M \\ \beta_M & -i\beta \end{pmatrix}. \tag{19}$$

According to the factorization of $r(E)$, the system can be understood in terms of $H^{abs}$,

$$H^{abs} = \begin{pmatrix} -i\beta & \beta_M \\ \beta_M & -i\beta \end{pmatrix}, \tag{20}$$

and $H^{trns}$

$$H^{trns} = \begin{pmatrix} i\beta & \beta_M \\ \beta_M & -i\beta \end{pmatrix}. \tag{21}$$

The eigenvectors and eigenvalues of $H^{abs}$ are given by

$$E_{1,2} = \pm\beta_M - i\beta, \tag{22}$$

$$v_{1,2} = (\pm 1, 1). \tag{23}$$

The eigenvectors describe the bond and an anti-bond, both of which are decaying into the continua of the contacts. The matrix $H^{trns}$ in this example is identical to the NH Hamiltonian matrix in Eq. (2) of Sec. I, exhibiting an exceptional point upon variation of the parameter $\beta$. The SSP model of a diatomic conductor provides the most immediate realization of the textbook NH Hamiltonian, which can hence be interpreted as a finite subsystem model of an infinite molecular electronic device. The eigenvectors and eigenvalues of $H^{trns}$ are given in Eqs. (3) and (4) of the Introduction. For $|\beta_M| > |\beta|$, these two eigenvectors represent a binding and an anti-binding orbital of real energy. For $|\beta_M| = |\beta|$, the two states coincide and the binding energy, i.e., the difference in the real parts of the energy between the molecule and the separated atoms, vanishes. This implies that the chemical bond between the atoms ceases to exist. This "bond breaking" is a manifestation of the exceptional point. The exceptional point is, however, a feature of $H^{trns}$ and it is not directly observable in a MED. Yet, there are observable consequences of attaining the exceptional point, which we describe now.

The primary quantity of interest of a MED is the transmission probability, it is related to the reflection coefficient through $T(E) = 1 - |r(E)|^2$, and it is proportional to the conductance $g(E) = (e^2/h) * T(E)$ of the MED. The transmission probability is investigated in Fig. 3, and the physical interpretation of the exceptional point is that of the coalescence of two resonances. As the size of the coupling of the molecule to the contacts ($|\beta|$) increases and approaches the size of the inter-atomic hopping ($|\beta_M|$), the two resonances in the transmission probability move toward each other to merge at the exceptional point. Further increase in $|\beta|$ leads to a reduction in the resonance height. Thus, the disappearance/emergence of a resonance as $|\beta|$ varies is an indicator for an exceptional point.

To further examine the exceptional point, in Fig. 3, we investigate the reflection coefficient $r$ as a function of the energy $E$. In the example studied, the exceptional point corresponds to the disappearance of one closed loop of the curve of $r$ in the complex plane. In Sec. V, we explain how $H^{trns}$ and its exceptional points are related to the winding number—a topological invariant of $r(E)$.

The Green's function approach to molecular conductance focuses on the transmission amplitude $t$ defined in Fig. 1. The Fischer–Lee formalism,[36] for instance, provides an expression for $t$ in terms of Green's functions. However, as we indicated already, the Green's function expression for $t$[39] does not relate exceptional points to molecular conductance.

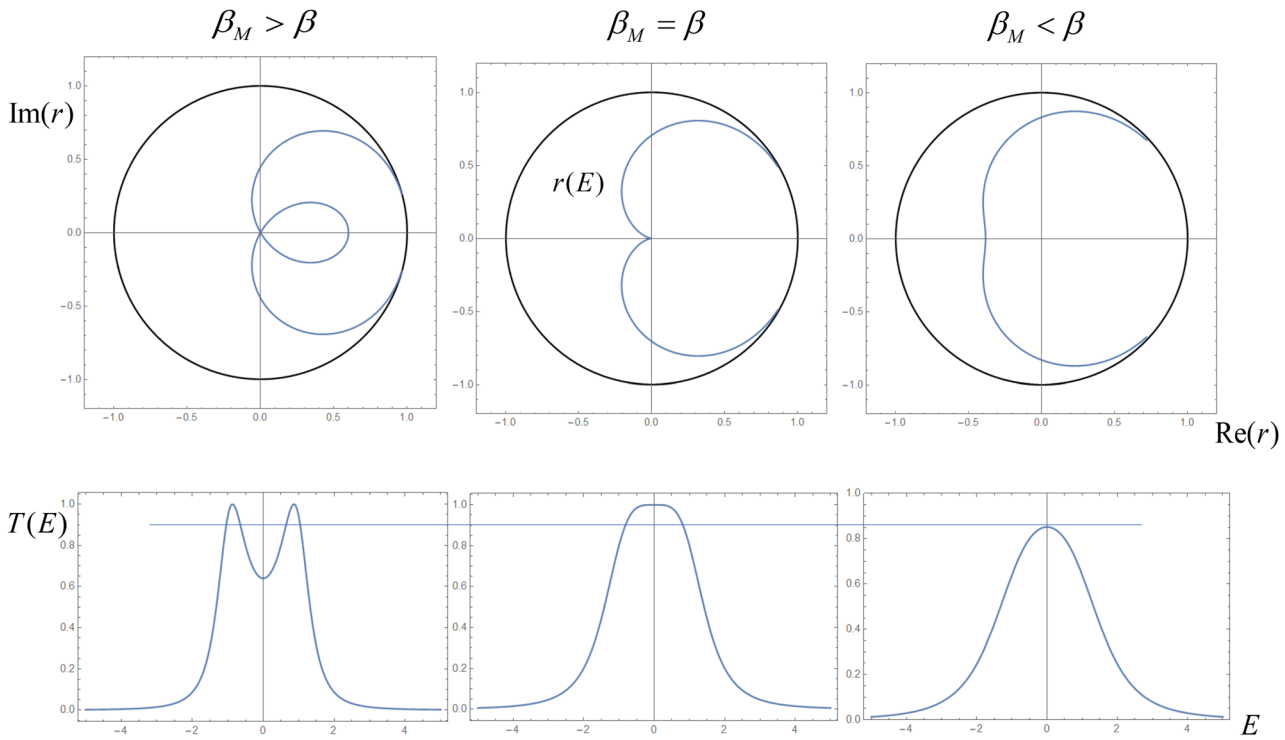


**FIG. 3**. Exceptional point in a molecular electronic device. The upper row shows the reflection coefficient $r(E)$ as a parametric function of the electron energy. For reference, a unit circle is added in each plot. The lower row shows the corresponding transmission probability $T(E)$. Three different values of $\beta$, describing the coupling of the molecule to the contacts, are considered ($\beta_M = 1$, $\beta = 0.5, 1, 1.5$). For $|\beta_M| > |\beta|$, there are two distinct maxima in $T(E)$, and correspondingly, $r(E)$ completes two loops in the complex plane. For $|\beta_M| = |\beta|$, the matrix $H^{trns}$ exhibits an exceptional point where the two molecular resonances coalesce. The exceptional point is characterized by the merging of the maxima in $T(E)$ and by the vanishing of one of the loops in $r(E)$. For $|\beta_M| < |\beta|$, we obtain only one maximum in $T(E)$, which does not reach one and diminishes further for increasing $|\beta|$.

## IV. EXCEPTIONAL POINT IN A DIATOMIC MOLECULE CONNECTED TO A SURFACE

The formalism presented thus far is now adapted to describe the resonance states of a molecule attached to a surface. The sketch in Fig. 2 depicts the system that we describe with the SSP model. There are two equivalent ways to apply SSP to this system: one it to remove the left contact from the MED built from a diatomic molecule by setting $\beta_L = 0$. This route yields the Hamiltonian considered in Sec. II A. However, within SSP, it is more convenient to couple the diatomic to the left contact and to set $\beta_R = 0$. The NH operators $H^{trns}$ and $H^{abs}$ are then again the key ingredients for the analysis of the system. An alternative model of a diatomic attached to a surface has recently been described in Ref. 53 to explain the catalytic bond dissociation on surfaces. For the problem at hand, $H^{trns}$ is given by

$$H^{trns} = \begin{pmatrix} i\beta & \cdots \\ \cdots & \cdots \end{pmatrix}. \tag{24}$$

The dotted part of the matrix is not essential for the present discussion, and it contains only real elements, arranged to form a symmetric matrix. Because the sink potential vanishes, $H^{abs} = H^{trns*}$ and $|r(E)| = 1$. This is not surprising since the electron cannot escape into the right contact. The eigenvalues and eigenvectors of $H^{trns}$ are given by

$$\begin{aligned} E_{1,2} &= \frac{1}{2}\left(\mp\sqrt{4{\beta_M}^2 - \beta^2} + i\beta\right), \\ v_{1,2} &= \left(\frac{\mp\sqrt{4{\beta_M}^2 - \beta^2} + i\beta}{2\beta_M}, 1\right). \end{aligned} \tag{25}$$

An exceptional point is realized for $|\beta| = 2|\beta_M|$, where the eigenvalues and eigenvectors (for $\beta = 2\beta_M$) are

$$\begin{aligned} E_{1,2} &= \frac{i\beta}{2}, \\ v_{1,2} &= (i, 1). \end{aligned} \tag{26}$$

In Fig. 4, the eigenvalues are plotted as a function of the parameter $\beta$. For $|\beta| < 2|\beta_M|$, there are two resonances whose energies have different real parts and identical imaginary parts. These resonances correspond to the binding and anti-binding orbital, both accumulating density from the contact. For $|\beta| = 2|\beta_M|$, the eigenvectors and eigenvalues coalesce. Beyond this $|\beta|$ value, the real part of the energies is zero, and there are two distinct imaginary energies that

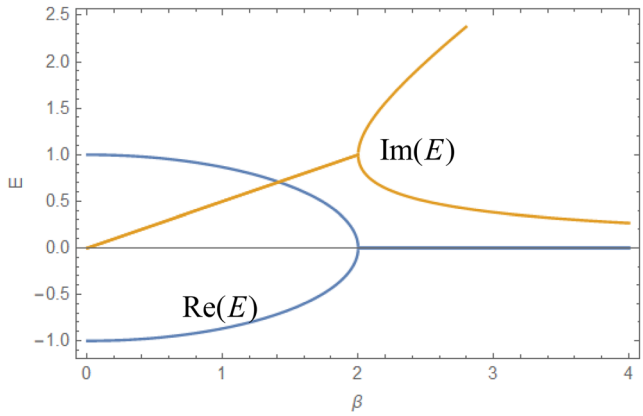


**FIG. 4**. The eigenvalues of the model Hamiltonian describing the diatomic molecule coupled to a surface. $\beta_M$ is arbitrarily set to one. Starting from zero, as $|\beta|$ increases, the separation between the binding and anti-binding orbital decreases. Approaching the exceptional point $|\beta| = 2|\beta_M|$, the rate of change $dE/d\beta$ goes to infinity. At the exceptional point, the real part of the eigenvalues vanishes and stays zero for further growing $|\beta|$, whereas the imaginary parts become increasingly distinct. The imaginary parts indicate that there are now two decay rates, one for the atom closest to the surface and the second one for the atom furthest to the surface.

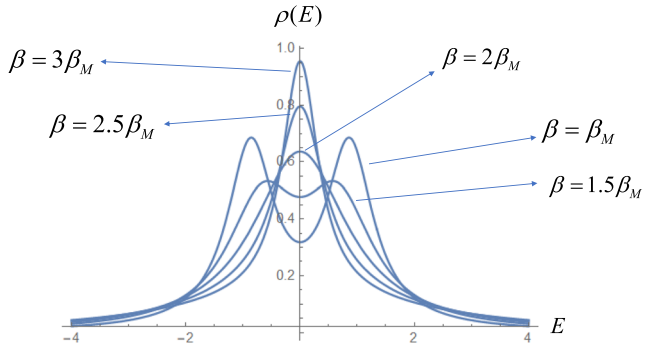


**FIG. 5**. Density of states on the diatomic molecule attached to a surface. $\beta_M$ is arbitrarily set to one. For values of the coupling ($|\beta|$) to the surface that are small in relation to $2|\beta_M|$, there are two maxima in the density of states. As $|\beta|$ increases, the maxima move toward each other and merge at the exceptional point $|\beta| = 2|\beta_M|$. Increasing $|\beta|$ further leads to an increased height of the maximum of the density of states. This is because one of the eigenvalues in Fig. 4 moves toward the real axis as $|\beta| \to \infty$, generating a delta-function contribution to the density of states.

separate further as $|\beta|$ grows. These eigenvalues describe a molecule separated into two distinct atoms, each with its own lifetime.

Again, complex energies cannot be realized, but an experimental observable quantity that can reveal the presence of an exceptional point is the local density of states on the molecule, which is obtained using Friedel's sum rule[54] $\rho(E) = \frac{1}{2\pi i} d\ln(\mathrm{Det}[S])/dE$. The scattering matrix $S$ has only one non-trivial element for the diatomic on the surface, i.e., $S = \left(\begin{smallmatrix} r & 0 \\ 0 & -1 \end{smallmatrix}\right)$. Since $H^{abs} = H^{trns*}$ and $|r| = 1$, this leads to

$$\rho(E) = \frac{1}{\pi} \frac{dArg(\mathrm{Det}[H^{trns} - E])}{dE}, \tag{27}$$

where $Arg(z)$ denotes the phase of $z$. In Fig. 5, the local density of states on the diatomic is shown. As expected, based on the discussion of the eigenvalues in Fig. 4, for $|\beta| = 2|\beta_M|$, there is an exceptional point of $H^{trns}$ where the two maxima in $\rho(E)$ join to form a broad one. Increasing $|\beta|$ further increases the maximum value of $\rho(E)$. Similar to what we observed for the diatomic conductor, the exceptional point marks a transition where the system separates into two subsystems, one consists of the topmost atom that acquires its own lifetime and it is linked to the atom-on-the-surface system, which has a shorter lifetime. We note that the physics of this molecular system is related to that of a damped classical harmonic oscillator, which also presents damped (corresponding to $|\beta| < 2|\beta_M|$) and over damped (corresponding to $|\beta| > 2|\beta_M|$) regimes separated by a critical regime, which is at the exceptional point. Indeed, exceptional points have recently been found in classical electrical resonators.[55]

Closing this section, we point out that the example of a molecule on a surface can also be treated within the Green's function approach and that the model Hamiltonian in this case is given by the one in Fig. 2 (cf. Ref. 39); it is equivalent to $H^{abs}$. Since $H^{abs} = H^{trns*}$, analogous conclusions hold for both Hamiltonians.

## V. WINDING NUMBER OF THE REFLECTION COEFFICIENT AND ITS RELATION TO THE EIGENVALUES OF $H^{trns}$

The reflection coefficient $r$ determines the transmission probability through its absolute value. The remaining information contained in $r(E) = |r(E)|e^{i\phi(E)}$ is the phase $\phi(E)$, which varies as a function of the energy. Since $r = 1$ for $E = \pm\infty$, the reflection coefficient as a function of $E$ describes a closed curve in the complex plane. A characteristic property of $\phi(E)$ is its winding number $N_W$, and it counts the number of closed circles around zero that are traced by $r(E)$. An illustration of a case with $N_W = 1$ can be found in the right panel of Fig. 3. In the left and middle panel, $r$ passes through zero, and in this case, $N_W$ is undefined. The winding number can be calculated according to

$$N_W = \frac{1}{2\pi} \oint d\phi \tag{28}$$

$$= \frac{1}{2\pi i} \oint \frac{dr}{r}. \tag{29}$$

The latter equation holds because $dr = d|r|e^{i\phi} + i|r|e^{i\phi}d\phi$, and therefore,

$$\frac{dr}{r} = \frac{d|r|}{|r|} + id\phi = d\ln|r| + id\phi. \tag{30}$$

The integral of $d\ln|r|$ over a closed loop vanishes so that only the integral over $id\phi$ remains. Using the residue theorem of complex analysis and applying it to the following energy integral, the winding number becomes

$$\frac{1}{2\pi i}\oint \frac{dr}{r} = \frac{1}{2\pi i}\int_{-\infty}^{+\infty} \frac{dr(E)}{r(E)dE}dE \tag{31}$$

$$= \sum_{i}^{N} \Theta(\mathrm{Im}(E_i^{trns})), \tag{32}$$

where the integration path over $E$ is closed with a demi-circle in the upper half of the complex plane at $|E| = \infty$, where $\frac{dr(E)}{r(E)dE} = 0$. The sum over the Heaviside step functions in this equation [$\Theta(x) = 1$ for $x > 1$ and $\Theta(x) = 0$ for $x < 1$] yields the number of eigenvalues of $H^{trns}$ in the upper half of the complex plane. In Fig. 6, we consider the simplest example of how the winding number changes as a function of the coupling of the system to the external contacts. As this example shows, the winding number reveals which contact, right or left, couples stronger to the molecule. If an orbital of the molecule is primarily coupled to the left contact, the corresponding eigenvalue of $H^{trns}$ is located in the upper-half plane, implying an accumulation of density on the molecule. The resonance ($r = 0$) marks the transition to a decaying state that is characterized by a finite lifetime due to the strong coupling to the right contact.

Another example for a changing winding number is provided by the diatomic conductor studied in Fig. 3. For $|\beta_M| \geq |\beta|$, the winding number is undefined since $r(E)$ passes through zero. As the coupling to the contacts is increased and passes through $|\beta| = |\beta_M|$, the two real eigenvalues of the corresponding $H^{trns}$ become purely imaginary, forming a complex conjugate pair. One of these eigenvalues lies in the upper half of the complex plain, resulting in a winding number of one, as is clearly observable in Fig. 3. The corresponding state describes the left atom of the molecule coupled predominantly to the left contact and accumulating probability density.

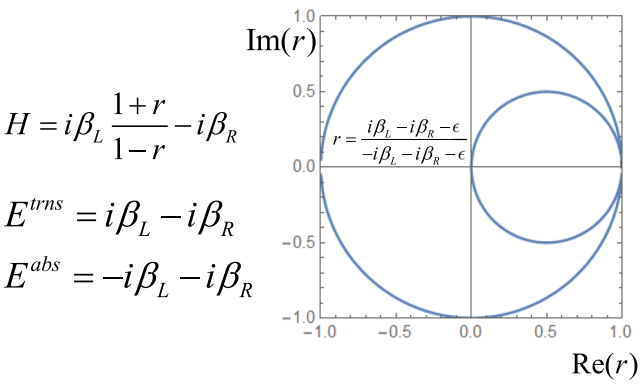


**FIG. 6.** The winding number $N_W$ and its relation to the eigenvalues of $H^{trns}$. We consider an atom coupled to contacts as described by the one-dimensional Hamiltonian in the upper left corner. The position of the eigenvalue $E^{trns}$ of $H^{trns}$ is a function of the coupling parameters to the left ($\beta_L$) and right contact ($\beta_R$). Starting with $E^{trns}$ in the upper half of the complex plane, i.e., $\beta_L > \beta_R$, so that $N_W = 1$, as $\beta_R$ is increased, the accumulation of density in the atom is reduced until a stationary state is reached where the current entering the atom is equal to the current leaving the atom. At this point, the eigenvalue of $H^{trns}$ becomes zero and $r(E = 0) = 0$ so that $N_W$ is undefined. Increasing $\beta_R$ further breaks the balance between incoming and outgoing current and the imaginary part of the energy diminishes, indicating a decrease in lifetime of the metastable state. In this regime, $N_W = 0$. In the right panel, the corresponding reflection coefficient is shown, illustrating the change in $N_W$ for varying values of $\beta_R$. The unit circle is obtained for $\beta_R = 0$, and increasing the value of $\beta_R$ reduces the radius of the circle until it passes through zero where $\beta_L = \beta_R$. For $\beta_L < \beta_R$, the radius diminishes further until it becomes zero because $r(E) = 1$ for all energies if $\beta_L$ is negligible compared to $\beta_R$.

## VI. CONCLUSION

The properties of quantum systems, which are always described by real-valued observables, can often be better understood by considering complex values of observables such as the energy. For instance, it is well known that a resonance of a molecule that is embedded in a continuum of states can be described by a single Siegert state[1,2,56] of complex energy. Relevant properties of the system, such as its lifetime, can then be inferred from the imaginary part of the Siegert energy.

In the present work, we review how a continuation of Hamiltonians depending on $r(E)$ into the complex energy plane can simplify the description of MEDs. The eigenvectors of $H^{abs}$ are the analogue to Siegert states, whereas the eigenvectors of $H^{trns}$ represent a generalization of the Siegert states and they provide a new link between NHQM and physical systems. Together, $H^{abs}$ and $H^{trns}$ describe a physical continuum of states in terms of discrete states with eigenvalues in the complex plane. The properties of $H^{trns}$ are closely related to the reflection coefficient of the corresponding MED; for instance, the number of eigenvalues of $H^{trns}$ in the upper-half of the complex plane yields the winding number of $r(E)$, a topological characteristic of $r(E)$; its physical interpretation is whether the eigenstates are predominately coupled to the left or the right contact.

In the case of a MED built with a dimer, as described here, the system exhibits inversion symmetry and the corresponding $H^{trns}$ is an example of a NH, parity, and time inversion symmetric Hamiltonian. This simple NH Hamiltonian matrix, which serves as a textbook example in NHQM, is thus directly related to the diatomic conductor. Therefore, the salient features of NHQM, such as the appearance of exceptional points, can be directly linked to observable phenomena in MEDs. Similarly, for molecules bound to surfaces, an important property is the spectral density of the molecular system, and again, exceptional points are clearly identifiable through it.

## ACKNOWLEDGMENTS

The financial support provided by the NSERC is gratefully acknowledged.

## DATA AVAILABILITY

The data that support the findings of this study are available within the article.

## REFERENCES

[1] R. Santra and L. S. Cederbaum, Phys. Rep. **368**, 1 (2002).
[2] N. Moiseyev, *Non-Hermitian Quantum Mechanics* (Cambridge University Press, 2011).
[3] I. Rotter and J. P. Bird, Rep. Prog. Phys. **78**, 114001 (2015).
[4] R. El-Ganainy, K. G. Makris, M. Khajavikhan, Z. H. Musslimani, S. Rotter, and D. N. Christodoulides, Nat. Phys. **14**, 11 (2018).

[5]A. Pick, P. R. Kaprálová-Žďánská, and N. Moiseyev, J. Chem. Phys. **150**, 204111 (2019).
[6]A. F. White, E. Epifanovsky, C. W. McCurdy, and M. Head-Gordon, J. Chem. Phys. **146**, 234107 (2017).
[7]E. Narevicius and N. Moiseyev, J. Chem. Phys. **113**, 6088 (2000).
[8]Y. Zhou and M. Ernzerhof, J. Phys. Chem. Lett. **3**, 1916 (2012).
[9]T.-C. Jagau and A. I. Krylov, J. Chem. Phys. **144**, 054113 (2016).
[10]T.-C. Jagau, K. B. Bravaya, and A. I. Krylov, Annu. Rev. Phys. Chem. **68**, 525 (2017).
[11]W. Skomorowski and A. I. Krylov, J. Phys. Chem. Lett. **9**, 4101 (2018).
[12]M. Ernzerhof, J. Chem. Phys. **125**, 124104 (2006).
[13]H. G. A. Burton, A. J. W. Thom, and P.-F. Loos, J. Chem. Phys. **150**, 041103 (2019).
[14]H. G. A. Burton, A. J. W. Thom, and P.-F. Loos, J. Chem. Theory Comput. **15**, 4374 (2019).
[15]K. Higuchi, Y. Fujie, H. Shimizu, and M. Higuchi, Phys. Rev. A **100**, 062503 (2019).
[16]J. Linderberg and Y. Öhrn, *Propagators in Quantum Chemistry* (John Wiley & Sons, 2004).
[17]G. Stefanucci and R. van Leeuwen, *Nonequilibrium Many-Body Theory of Quantum Systems: A Modern Introduction* (Cambridge University Press, 2013).
[18]L. Reining, Wiley Interdiscip. Rev.: Comput. Mol. Sci. **8**, e1344 (2018).
[19]R. El-Ganainy, M. Khajavikhan, D. N. Christodoulides, and S. K. Ozdemir, Commun. Phys. **2**, 37 (2019).
[20]M. Müller and I. Rotter, J. Phys. A: Math. Theor. **41**, 244018 (2008).
[21]I. Haritan, I. Gilary, Z. Amitay, and N. Moiseyev, J. Chem. Phys. **143**, 154308 (2015).
[22]W. D. Heiss, in *Non-Hermitian Hamiltonians in Quantum Physics*, edited by F. Bagarello, R. Passante, and C. Trapani (Springer International Publishing, Cham, 2016), pp. 281–288.
[23]C. M. Bender, Contemp. Phys. **46**, 277 (2005).
[24]S. Datta, H. Ahmad, and M. Pepper, *Electronic Transport in Mesoscopic Systems*, Cambridge Studies in Semiconductor Physics and Microelectronic Engineering (Cambridge University Press, 1997).
[25]J. P. Bergfield and M. A. Ratner, Phys. Status Solidi B **250**, 2249 (2013).
[26]R. M. Metzger, Chem. Rev. **115**, 5056 (2015).
[27]D. Xiang, X. Wang, C. Jia, T. Lee, and X. Guo, Chem. Rev. **116**, 4318 (2016).
[28]T. A. Su, M. Neupane, M. L. Steigerwald, L. Venkataraman, and C. Nuckolls, Nat. Rev. Mater. **1**, 16002 (2016).
[29]P. Gehring, J. M. Thijssen, and H. S. J. van der Zant, Nat. Rev. Phys. **1**, 381 (2019).
[30]N. Xin, J. Guan, C. Zhou, X. Chen, C. Gu, Y. Li, M. A. Ratner, A. Nitzan, J. F. Stoddart, and X. Guo, Nat. Rev. Phys. **1**, 211 (2019).
[31]J. C. Cuevas and E. Scheer, *Molecular Electronics: An Introduction to Theory and Experiment*, World Scientific Series in Nanoscience and Nanotechnology, 2nd ed. (World Scientific Publishing Company, 2017).
[32]A. A. Gorbatsevich and N. M. Shubin, JETP Lett. **103**, 769 (2016).
[33]A. A. Gorbatsevich and N. M. Shubin, Ann. Phys. **376**, 353 (2017).
[34]A. A. Gorbatsevich, G. Y. Krasnikov, and N. M. Shubin, Sci. Rep. **8**, 15780 (2018).
[35]L.-L. Zhang, G.-H. Zhan, D.-Q. Yu, and W.-J. Gong, Superlattices Microstruct. **113**, 558 (2018).
[36]D. S. Fisher and P. A. Lee, Phys. Rev. B **23**, 6851 (1981).
[37]V. Mujica, M. Kemp, and M. A. Ratner, J. Chem. Phys. **101**, 6849 (1994).
[38]V. Mujica, M. Kemp, and M. A. Ratner, J. Chem. Phys. **101**, 6856 (1994).
[39]L. E. Hall, J. R. Reimers, N. S. Hush, and K. Silverbrook, J. Chem. Phys. **112**, 1510 (2000).
[40]M. Ernzerhof, J. Chem. Phys. **127**, 204709 (2007).
[41]F. Goyer, M. Ernzerhof, and M. Zhuang, J. Chem. Phys. **126**, 144104 (2007).
[42]B. T. Pickup and P. W. Fowler, Chem. Phys. Lett. **459**, 198 (2008).
[43]F. Goyer and M. Ernzerhof, J. Chem. Phys. **134**, 174101 (2011).
[44]P. W. Fowler, B. T. Pickup, and T. Z. Todorova, Pure Appl. Chem. **83**, 1515 (2011).
[45]P. Rocheleau and M. Ernzerhof, J. Chem. Phys. **137**, 174112 (2012).
[46]D. Mayou, Y. Zhou, and M. Ernzerhof, J. Phys. Chem. C **117**, 7870 (2013).
[47]B. T. Pickup, P. W. Fowler, M. Borg, and I. Sciriha, J. Chem. Phys. **143**, 194105 (2015).
[48]A. Giguère, M. Ernzerhof, and D. Mayou, J. Phys. Chem. C **122**, 20083 (2018).
[49]P. W. Fowler, M. Borg, B. T. Pickup, and I. Sciriha, Phys. Chem. Chem. Phys. **22**, 1349 (2020).
[50]Y. Zhou and M. Ernzerhof, J. Chem. Phys. **136**, 094105 (2012).
[51]S. Fias and T. Stuyver, J. Chem. Phys. **147**, 184102 (2017).
[52]M. Ernzerhof and M. Zhuang, J. Chem. Phys. **119**, 4134 (2003).
[53]A. Ruderman, A. D. Dente, E. Santos, and H. M. Pastawski, J. Phys.: Condens. Matter **27**, 315501 (2015).
[54]H.-W. Lee, Phys. Rev. Lett. **82**, 2358 (1999).
[55]Y. Choi, C. Hahn, J. W. Yoon, and S. H. Song, Nat. Commun. **9**, 2182 (2018).
[56]A. J. F. Siegert, Phys. Rev. **56**, 750 (1939).